Structural Engineering and Mechanics, Vol. 13, No. 2 (2002) 135-154
DOI: http://dx.doi.org/10.12989/sem.2002.13.2.135

Large displacement analysis of inelastic frame structures by convected material frame approach

Yaw-Jeng Chiou†

Department of Civil Engineering, National Cheng Kung University, Tainan, Taiwan 701, R.O.C.

Yeon-Kang Wang‡

Department of Civil Engineering, Chung-Cheng Institute of Technology, National Defense University, Taoyuan, Taiwan 335, R.O.C.

Pang-An Hsiao and Yi-Lung Chen‡†

Department of Civil Engineering, National Cheng Kung University, Tainan, Taiwan 701, R.O.C.

Abstract. This paper presents the convected material frame approach to study the nonlinear behavior of inelastic frame structures. The convected material frame approach is a modification of the co-rotational approximation by incorporating an adaptive convected material frame in the basic definition of the displacement vector and strain tensor. In the formulation, each discrete element is associated with a local coordinate system that rotates and translates with the element. For each load increment, the corresponding strain-displacement and nodal force-stress relationships are defined in the updated local coordinates, and based on the updated element geometry. The rigid body motion and deformation displacements are decoupled for each increment. This modified approach incorporates the geometrical nonlinearities through the continuous updating of the material frame geometry. A generalized nonlinear function is used to derive the inelastic constitutive relation and the kinematic hardening is considered. The equation of motion is integrated by an explicit procedure and it involves only vector assemblage and vector storage in the analysis by assuming a lumped mass matrix of diagonal form. Several numerical examples are demonstrated in close agreement with the solutions obtained by the ANSYS code. Numerical studies show that the proposed approach is capable of investigating large deflection of inelastic planar structures and providing an excellent numerical performance.

Key words: convected material frame approach; explicit finite element analysis; inelastic frame structures.

1. Introduction

Large displacement analysis of elastic structures has been extensively studied. Many researchers presented explicit algorithms for finite element analysis. Belytschko and Hsieh (1973), Belytschko

† Professor
‡ Associate Professor
‡† Graduate student

et al. (1977) formulated the frame elements by using the traditional co-rotational approach. Belytschko and Marchertas (1974) formulated the three-dimensional plate element following a similar approach. Hsiao *et al.* (1987) presented the large rotations of spatial beam structures. They removed the restriction of small rotations of space frames by using a co-rotational procedure and incremental-iterative methods. Crisfield (1990) proposed a co-rotational formulation for three-dimensional beams in which both the internal force vector and tangent stiffness matrix are consistently derived from the adopted strains. The adopted strains related to conventional small-deflection beam theory but were embedded in a continuously rotating frame. Rice and Ting (1993) proposed an approach of updated geometry to develop a plane frame analysis procedure. However, their element stiffness is obtained by a direct stiffness approach and Castigliano's theorem. Hence, the formulation is restricted to prismatic frame elements and linearly elastic materials. Wang *et al.* (1998) formulated a general curved elastic frame element based on a convected material frame approach, and developed a general explicit algorithm for the analysis of flexible structures subjected to large geometry changes. This approach is a modification of the co-rotational approximation by incorporating an adaptive convected material frame in the basic definition of the displacement vector and strain tensor. Recently, Hsiao *et al.* (1999) developed a consistent co-rotational total Lagrangian finite element for the geometrically nonlinear dynamic analysis of spatial Euler beam with large rotations but small strain. Element deformations and element equations are defined in terms of element coordinates, which are constructed at the current configuration of the beam element. In conjunction with the co-rotational formulation, the higher-order terms of nodal parameters in element nodal force and stiffness matrix are consistently dropped.

Researchers also have extensively studied the structures with nonlinear materials. Tang *et al.* (1980) adopted the traditional co-rotational approach and bi-linear constitutive relation to analyze the large deflection of the plane frame. Yang and Saigal (1984) studied the static and dynamic response of beam with bi-linear material and large deflection. Dafalis (1987, 1988) analyzed the kinematics and kinetics at large elastoplastic deformations within the framework of a general macroscopic constitutive theory with tensorial structure variables. The important coupling between kinematics and kinetics had been introduced by defining the meaning of the co-rotational and corodeformational rates of the structure variables. Wang *et al.* (1995) proposed a numerical model to study the large deflection of an elastoplastic cantilever. They divided the deformed axis into a number of small segments and assumed each segment to be approximated as a circular arc. Recently, Mamaghani *et al.* (1996) developed an elastoplastic finite element formulation for beam-columns to analyze the structural steel members under cyclic loading. They used the modified approximate updated Lagrangian description of motion to study the geometrical nonlinearity. The two-surface plasticity model is employed for material nonlinearity.

The convected material frame approach (Wang *et al.* 1998) is applied in this study to investigate the geometrical nonlinearity of inelastic frame structures. The inelastic constitutive relation is derived by using a generalized nonlinear function and the kinematic hardening is adopted to account for the Bauschinger effect. In the following, the formulation of the explicit finite element method based on a convected material frame approach is presented first. The algorithm is then verified by comparing the numerical solutions with the results obtained by the ANSYS code (1998) of the finite element method, and the nonlinear behavior of an inelastic frame is fully studied.

2. Formulation of the convected material frame approach

The convected material frame approach (Wang *et al.* 1998) is a modification of the co-rotational approximation by incorporating an adaptive convected material frame in the basic definition of the displacement vector and strain tensor. In the formulation, each discrete element is associated with a local coordinate system. For each load increment, the local coordinate system assumes a new orientation and the element geometry also assumes a new shape. The corresponding strain-displacement and nodal force-stress relationships are defined in the updated local coordinates, and based on the updated element geometry. The rigid body motion and deformation displacement are decoupled for each increment. The nonlinearities associated with the large geometrical changes are incorporated in the analysis through the continuous updating of the material frame geometry. By assuming a lumped mass matrix of diagonal form, the explicit finite element analysis involves only vector assemblage and vector storage.

2.1 Coordinates

Referring to Fig. 1(a), the traditional co-rotational approach decomposes the displacement history

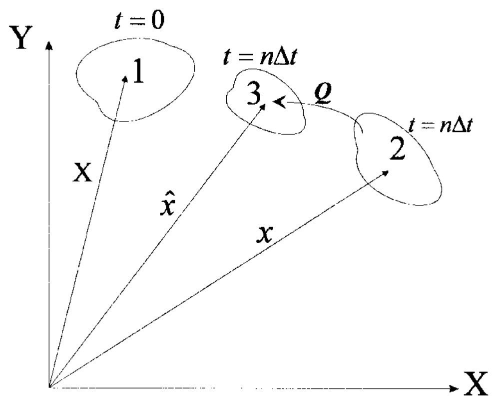

Fig. 1 (a) Schematic description of the traditional co-rotational approach

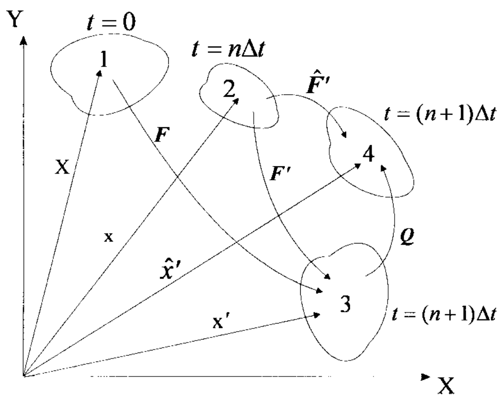

Fig. 1 (b) Schematic description of the convected material reference frame into three stages (Rice and Ting 1993): (1) the initial geometry $\boldsymbol{X}$ at the reference time $t = 0$, (2) the current deformed geometry $\boldsymbol{x}$ at time $t = n\Delta t$, (3) the convected geometry $\hat{\boldsymbol{x}}$ at the same time as in stage 2. This approach is based on the premise that each element has its own local coordinate $\hat{\boldsymbol{x}}$, which rotates and translates with the element throughout its load-displacement history. The rigid body motion is represented by the $\boldsymbol{Q}$ matrix. The convected material frame approach is a modified co-rotational approach, and adopts the updated geometry. Its displacement history of a body subjected to large displacement is decomposed into four stages Fig. 1b: (1) the initial geometry $\boldsymbol{X}$ at the reference time $t = 0$, (2) the convected material reference frame $\boldsymbol{x}$ at time $t = n\Delta t$, (3) the deformed body geometry $\boldsymbol{x}'$ at time $t' = (n+1)\Delta t$, and (4) the convected geometry $\hat{x}'$ at time t'. The convected geometry $\hat{x}'$ is related to the deformed body geometry $\boldsymbol{x}'$ by a pure rotation $\boldsymbol{Q}$.

2.2 Kinematics

Fig. 2 shows a segment of a curved frame element under loading. The section *EFGH*, the radius of curvature *R*, and the central angle $d\theta$ describe the element material geometry $\boldsymbol{x}$ at time *t*, while section $E'F'G'H'$, R', and $d\theta'$ describe the element convected geometry $\boldsymbol{x}'$ at time t'.

The frame element is assumed to follow the Bernoulli-Euler beam theory. The thickness and width of the frame element are small compared to the element length. The effect of Poisson's ratio is negligible, and the dimensions of the cross section remain unchanged. When the geometry changes from $\boldsymbol{x}$ to the $\boldsymbol{x}'$, a plane cross section of the element remains to be a plane. In addition, it is assumed that the strain for each load increment is small, but total strain can be large.

Referring to Fig. 2, the axial strain in the fiber $C'D'$ can be written as

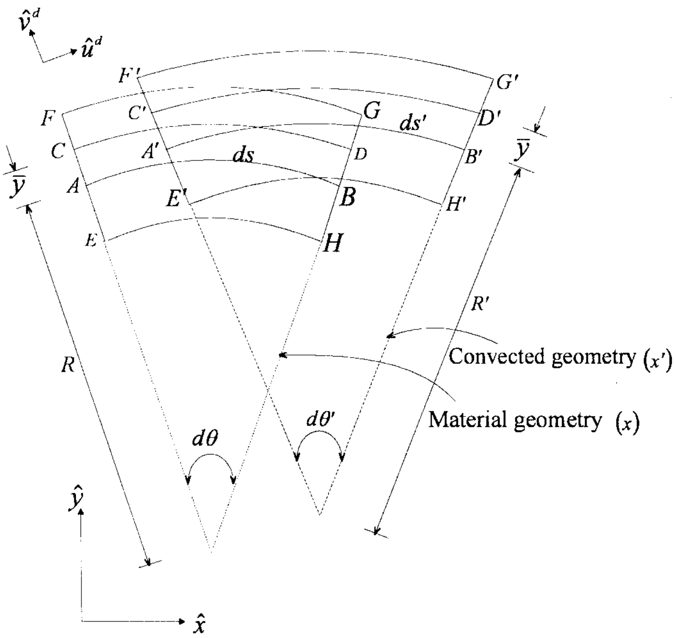

Fig. 2 Kinematics for normal strain

$$\hat{\varepsilon} = \frac{1}{2}\left[\left(\frac{C'D'}{CD}\right)^2 - 1\right] \tag{1}$$

where

$$CD = \left(1 + \frac{\bar{y}}{R}\right)ds$$

$$C'D' = \left(1 + \frac{\bar{y}}{R'}\right)ds'$$

The frame thickness is assumed to be small compared to the radius of curvature, or

$$\frac{\bar{y}}{R} \quad \text{and} \quad \frac{\bar{y}}{R'} << 1,$$

$\hat{\varepsilon}$ can then be simplified as

$$\hat{\varepsilon} \cong \hat{\varepsilon}_m + \bar{y}\Delta k \tag{2}$$

where $\hat{\varepsilon}_m$ is a uniform normal strain due to the change of the element length, and Δk is the change of the element curvature. Specific forms of $\hat{\varepsilon}_m$ and Δk are obtained by neglecting the higher order terms.

$$\hat{\varepsilon}_m = \frac{1}{2}\left[\left(\frac{ds'}{ds}\right)^2 - 1\right]$$

$$\cong \frac{\hat{v}^d}{R} + \frac{\partial \hat{u}^d}{\partial s} \tag{3}$$

$$\Delta k = \frac{1}{R'}\left(\frac{ds'}{ds}\right)^2 - \frac{1}{R}$$

$$\cong \left(\frac{\hat{v}^d}{R^2} + \frac{1}{R}\frac{\partial \hat{u}^d}{\partial s}\right) - \frac{\partial^2 \hat{v}^d}{\partial s^2} \tag{4}$$

where $\hat{u}^d$ and $\hat{v}^d$ are the longitudinal and transverse displacements in the convected coordinates (Fig. 3).

Fig. 4 shows a typical frame element, where s is the length measured, α_1 and α_2 the nodal slopes of the reference geometry, θ_1 and θ_2 the slope changes, l_0 and l the lengths of the element, l_m and l_n and the distances between nodes. The change of distance between two end nodes along $\hat{x}$-axis Δ, and the changes of end slopes of the element θ_1 and θ_2, are the independent nodal displacements.

The displacements are expressed in terms of the nodal displacements and written as

$$\hat{u}^d = L(s)\Delta \tag{5}$$

$$\hat{v}^d = N_1(s)\Delta + N_2(s)\theta_1 + N_3(s)\theta_2 \tag{6}$$

where

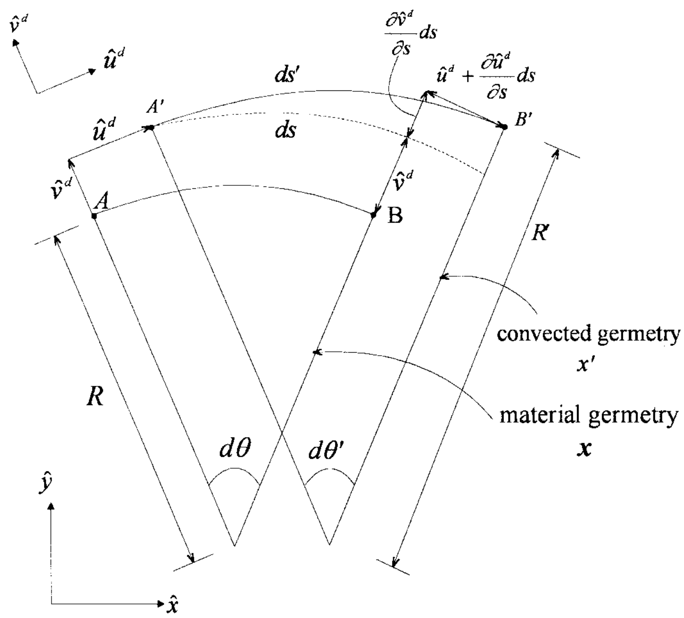

Fig. 3 (a) Kinematics for mid-plane strain-comparison of a segment in x and x'

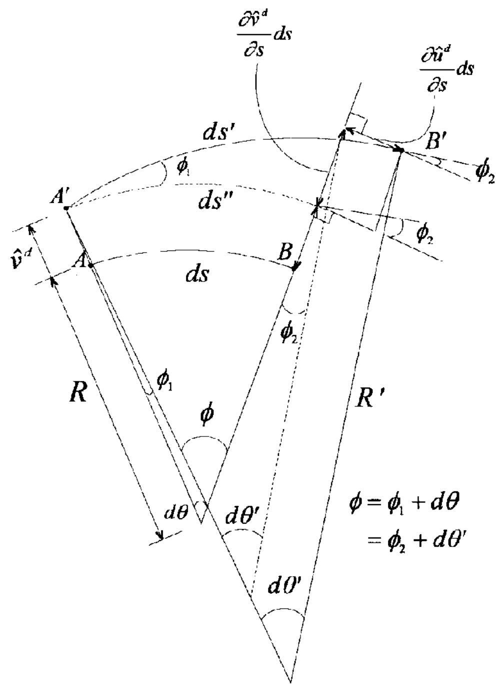

Fig. 3 (b) Kinematics for curvature variation-comparison of a segment in x and x' with removal of rigid-body displacement in $\hat{u}^d$ direction only

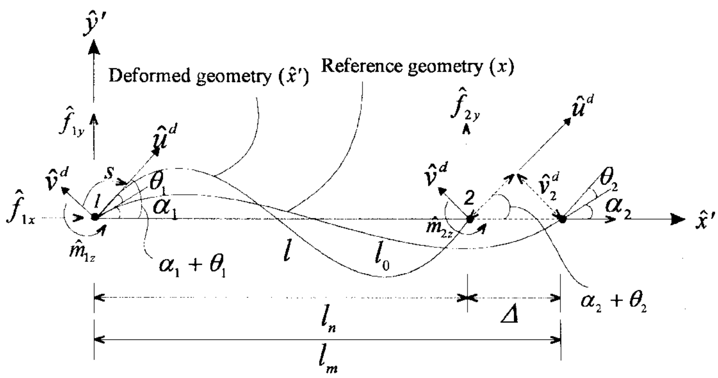

Fig. 4 Comparison of a curved frame element

$$L(s) = \frac{s}{l}\cos(\alpha_2 + \theta_2)$$

$$N_1(s) = \left(-3\frac{s^2}{l^2} + 2\frac{s^3}{l^3}\right)\sin(\alpha_2 + \theta_2)$$

$$N_2(s) = s - 2\frac{s^2}{l} + \frac{s^3}{l^2}$$

$$N_3(s) = -\frac{s^2}{l} + \frac{s^3}{l^2}$$

Substituting Eqs. (5) and (6) into Eqs. (3) and (4), the normal strain $\hat{\varepsilon}_m$ and the change of curvature Δk are thus expressed as

$$\begin{aligned} \hat{\varepsilon}_m &= [L_{,s} + N_1/R \quad N_2/R \quad N_3/R]\begin{bmatrix}\Delta \\ \theta_1 \\ \theta_2\end{bmatrix} \\ &= [B_{01} \quad B_{02} \quad B_{03}]\begin{bmatrix}\Delta \\ \theta_1 \\ \theta_2\end{bmatrix} \\ &= \boldsymbol{B}_0^T \hat{\boldsymbol{d}}_e^* \end{aligned} \tag{7}$$

$$\begin{aligned} \Delta k &= [N_1/R^2 - N_{1,ss} + L_{,s}/R \quad N_2/R - N_{2,ss} \quad N_3/R - N_{3,ss}]\begin{bmatrix}\Delta \\ \theta_1 \\ \theta_2\end{bmatrix} \\ &= [B_{r1} \quad B_{r2} \quad B_{r3}]\begin{bmatrix}\Delta \\ \theta_1 \\ \theta_2\end{bmatrix} \\ &= \boldsymbol{B}_r^T \hat{\boldsymbol{d}}_e^* \end{aligned} \tag{8}$$

2.3 Principle of virtual work

A structural system in the deformed geometry $\boldsymbol{x}'$, at time $t' = (n+1)\Delta t$, is said to be in equilibrium if it satisfies the virtual work formulation

$$\delta U = \delta W \tag{9a}$$

or

$$\sum_e \delta U_e = \sum_e \delta W_e \tag{9b}$$

where U is the internal work, W the external work, and e the number of elements. The total displacements are separated into the rigid-body displacements and the deformation displacements. Because the internal virtual work due to a virtual rigid-body motion is zero, the internal virtual work can then be expressed as

$$\begin{aligned}\delta U = \delta U^d &= \sum_e \delta U_e^d \\ &= \sum_e \int_{Ve} \delta \hat{\varepsilon}^T \hat{\sigma} \; dV\end{aligned} \tag{10}$$

where $\hat{\varepsilon}$ is the normal strain along the longitudinal direction, and $\hat{\sigma}$ the total longitudinal stress.

$$\hat{\sigma} = \hat{\sigma}^m + \hat{\sigma}' \tag{11}$$

where $\hat{\sigma}^m$ is the stress at the material frame geometry, and $\hat{\sigma}'$ the stress increment from $\boldsymbol{x}$ to $\hat{\boldsymbol{x}}'$.

$$\hat{\sigma}' = E\hat{\varepsilon} = E(\hat{\varepsilon}_m + \bar{y}\Delta k) \tag{12}$$

where $E = E(\varepsilon_j)$ is the tangent modulus, and it is a function of transverse coordinates $\bar{y}$.

$$E(\varepsilon_j) = \left.\frac{d\sigma}{d\varepsilon}\right|_{\varepsilon_j} = f'(\varepsilon_j) \tag{13}$$

where $f(\varepsilon)$ is a generalized nonlinear function used to derive the inelastic constitutive relation.

For a Bernoulli-Euller beam, the cross-sectional area is assumed to be unchanged throughout the deformation process. The internal work for each element is then

$$\begin{aligned}\delta U_e^d = \delta(\hat{\boldsymbol{d}}_e^*)^T \int_s \{ & (\boldsymbol{B}_0 P^m + \boldsymbol{B}_r M_z^m) + \\ & [(\int_A E dA)\boldsymbol{B}_0\boldsymbol{B}_0^T + (\int_A E\bar{y}^2 dA)\boldsymbol{B}_r\boldsymbol{B}_r^T]\hat{\boldsymbol{d}}_e^* + \\ & [(\int_A E\bar{y}\, dA)(\boldsymbol{B}_0\boldsymbol{B}_r^T + \boldsymbol{B}_r\boldsymbol{B}_0^T)]\hat{\boldsymbol{d}}_e^* \} ds\end{aligned} \tag{14}$$

or

$$\delta U_e^d = \delta(\hat{\boldsymbol{d}}_e^*)^T \hat{\boldsymbol{f}}_e^* = [\delta\Delta \quad \delta\theta_1 \quad \delta\theta_2] \begin{bmatrix} \hat{f}_{2x} \\ \hat{m}_{1z} \\ \hat{m}_{2z} \end{bmatrix} \tag{15}$$

where

$$P^m = \int_A \hat{\sigma}^m \, dA \tag{16a}$$

$$M_z^m = \int_A \hat{\sigma}^m \bar{y} \, dA \tag{16b}$$

$$\hat{\boldsymbol{f}}_e^* = \hat{\boldsymbol{f}}_e^m + \Delta \hat{\boldsymbol{f}}_e^* + \hat{\boldsymbol{f}}_e^n \tag{16c}$$

$$\hat{\boldsymbol{f}}_e^m = \int_s (\boldsymbol{B}_0 P^m + \boldsymbol{B}_r M_z^m) ds \tag{16d}$$

$$\begin{aligned} \Delta \hat{\boldsymbol{f}}_e^* &= \hat{\boldsymbol{k}}_e \hat{\boldsymbol{d}}_e^* \\ &= \{\int_s [(\int_A E dA)\boldsymbol{B}_0 \boldsymbol{B}_0^T + (\int_A E \bar{y}^2 dA)\boldsymbol{B}_r \boldsymbol{B}_r^T] ds\} \hat{\boldsymbol{d}}_e^* \end{aligned} \tag{16e}$$

$$\hat{\boldsymbol{f}}_e^n = \{\int_s [(\int_A E \bar{y} \, dA)(\boldsymbol{B}_0 \boldsymbol{B}_r^T + \boldsymbol{B}_r \boldsymbol{B}_0^T)] ds\} \hat{\boldsymbol{d}}_e^* \tag{16f}$$

The integration in Eq. (16) concerning the tangent modulus $E(\varepsilon_j)$ is performed by the Gaussian quadrature method in this study.

The element masses are lumped at the nodes. Each node is assumed to be in dynamic equilibrium while each element is in static equilibrium. The static equilibrium yields

$$\begin{aligned} \hat{f}_{1x} &= -\hat{f}_{2x} \\ \hat{f}_{1y} &= (\hat{m}_{1z} + \hat{m}_{2z})/l_n \\ \hat{f}_{2y} &= -\hat{f}_{1y} \end{aligned} \tag{17}$$

The full internal force and deformation displacement vectors for each element are

$$(\hat{\boldsymbol{f}}_e^{int})^T = [\hat{f}_{1x} \;\; \hat{f}_{1y} \;\; \hat{m}_{1z} \;\; \hat{f}_{2x} \;\; \hat{f}_{2y} \;\; \hat{m}_{2z}] \tag{18a}$$

$$\begin{aligned} (\hat{\boldsymbol{d}}_e^d)^T &= [\hat{d}_{1x}^d \;\; \hat{d}_{1y}^d \;\; \hat{\theta}_{1z} \;\; \hat{d}_{2x}^d \;\; \hat{d}_{2y}^d \;\; \hat{\theta}_{2z}] \\ &= [0 \;\; 0 \;\; \theta_1 \;\; \Delta \;\; 0 \;\; \theta_2] \end{aligned} \tag{18b}$$

The internal virtual work is thus given as

$$\delta U = \sum_e \delta U_e^d = \sum_e (\delta \hat{\boldsymbol{d}}_e^*)^T \hat{\boldsymbol{f}}_e^* = \sum_e (\delta \hat{\boldsymbol{d}}_e^d)^T \hat{\boldsymbol{f}}_e^{int} \tag{19}$$

Using the transformation matrix $\boldsymbol{T}$ between $\boldsymbol{x}$ and $\hat{\boldsymbol{x}}'$, one obtains

$$\hat{\boldsymbol{d}}_e = \boldsymbol{T} \boldsymbol{d}_e$$

Then

$$\delta U = \sum_e \delta \boldsymbol{d}_e^T \boldsymbol{f}_e^{int} \tag{20}$$

where

$$\boldsymbol{f}_e^{int} = \boldsymbol{T}^T \hat{\boldsymbol{f}}_e^{int}$$

is the internal nodal force vector for the element written in the global coordinates. The transformation matrix has the same form as the one given in the traditional co-rotational approach.

$$\boldsymbol{T} = \begin{bmatrix} \cos\theta & \sin\theta & 0 & 0 & 0 & 0 \\ -\sin\theta & \cos\theta & 0 & 0 & 0 & 0 \\ 0 & 0 & 1 & 0 & 0 & 0 \\ 0 & 0 & 0 & \cos\theta & \sin\theta & 0 \\ 0 & 0 & 0 & -\sin\theta & \cos\theta & 0 \\ 0 & 0 & 0 & 0 & 0 & 1 \end{bmatrix}$$

where θ is the angle between global axis X and the convected coordinate axis $\hat{x}'$.

The external virtual work is

$$\begin{aligned} \delta W &= \sum_e (\delta \boldsymbol{d}_e^T \boldsymbol{f}_e^{ext} - \delta \hat{\boldsymbol{d}}_e^T \hat{\boldsymbol{M}}_e \ddot{\hat{d}}_e) \\ &= \sum_e (\delta \boldsymbol{d}_e^T \boldsymbol{f}_e^{ext} - \delta \boldsymbol{d}_e^T \boldsymbol{T}^T \hat{\boldsymbol{M}}_e \boldsymbol{T} \ddot{d}_e) \\ &= \sum_e \delta \boldsymbol{d}_e^T (\boldsymbol{f}_e^{ext} - \boldsymbol{M}_e \ddot{\boldsymbol{d}}_e) \end{aligned} \tag{21}$$

where

$$\boldsymbol{f}_e^{ext} = \begin{bmatrix} f_{1x} \\ f_{1y} \\ m_{1z} \\ f_{2x} \\ f_{2y} \\ m_{2z} \end{bmatrix}, \quad \boldsymbol{M}_e = \begin{bmatrix} \hat{M}_{1x} & 0 & 0 & 0 & 0 & 0 \\ 0 & \hat{M}_{1y} & 0 & 0 & 0 & 0 \\ 0 & 0 & \hat{I}_{1z} & 0 & 0 & 0 \\ 0 & 0 & 0 & \hat{M}_{2x} & 0 & 0 \\ 0 & 0 & 0 & 0 & \hat{M}_{2y} & 0 \\ 0 & 0 & 0 & 0 & 0 & \hat{I}_{2z} \end{bmatrix}$$

with

$$\hat{M}_{1x} = \hat{M}_{1y} = \hat{M}_{2x} = \hat{M}_{2y} = \frac{1}{2}\rho A l$$

$$\hat{I}_{1z} = \hat{I}_{2z} = \frac{1}{24}\rho l (A l^2 + 12 I_z)$$

$$\rho = \text{mass density}$$

The principle of virtual work yields

$$\sum_e \delta \boldsymbol{d}_e^T \boldsymbol{f}_e^{int} = \sum_e \delta \boldsymbol{d}_e^T (\boldsymbol{f}_e^{ext} - \boldsymbol{M}_e \ddot{\boldsymbol{d}}_e) \tag{22}$$

If one introduces a global assembled nodal displacement vector $\boldsymbol{d}$, the above equation becomes

$$\delta \boldsymbol{d}^T \left(\sum_e \boldsymbol{f}_e^{int} \right) = \delta \boldsymbol{d}^T \left(\sum_e \boldsymbol{f}_e^{ext} \right) - \delta \boldsymbol{d}^T \left(\sum_e \boldsymbol{M}_e \right) \ddot{\boldsymbol{d}} \tag{23}$$

Since $\delta \boldsymbol{d}$ is arbitrary, the equation of motion in global coordinates yields

$$\boldsymbol{M} \ddot{\boldsymbol{d}} = \boldsymbol{F}^{ext} - \boldsymbol{F}^{int} \tag{24}$$

where

$$\boldsymbol{M} = \sum_e \boldsymbol{M}_e, \quad \boldsymbol{F}^{ext} = \sum_e \boldsymbol{f}_e^{ext}, \text{ and } \boldsymbol{F}^{int} = \sum_e \boldsymbol{f}_e^{int}$$

2.4 Explicit time integration

For a diagonal mass matrix $\boldsymbol{M}$, the acceleration of the j-th degree of freedom is

$$\ddot{d}_j = \frac{1}{M_j}(F_j^{ext} - F_j^{int}) \qquad j = 1, 2, 3, ..., n \tag{25}$$

where n is the number of the unknowns.

To find the quasi-static solution through a dynamic relaxation procedure, a damping force may be added.

$$\boldsymbol{M} \ddot{\boldsymbol{d}} = \boldsymbol{F}^{ext} - \boldsymbol{F}^{int} - \boldsymbol{F}^{dmp} \tag{26}$$

The damping force may be written by assuming a standard Rayleigh damping

$$\boldsymbol{F}^{dmp} = C\dot{\boldsymbol{d}} = (\alpha \boldsymbol{M} + \beta \boldsymbol{K})\dot{\boldsymbol{d}}$$

in which α and β are constants, and $\boldsymbol{K}$ is the global stiffness matrix. In this study, since the global stiffness matrix is not available in the formulation, β is assumed to be zero. Or

$$\boldsymbol{F}^{dmp} = \alpha \boldsymbol{M} \dot{\boldsymbol{d}} \tag{27}$$

The assumption of β to be zero is only for the purpose of convenience to obtain the quasi-static solutions, and there is no physical meaning. The explicit time integration method is adopted to solve the equation and a second order central difference formulation is used as the time integration technique.

$$\boldsymbol{d}_{i+1} = \left(\frac{2}{2 + \alpha \Delta t} \right) \Delta t^2 \boldsymbol{M}^{-1} (\boldsymbol{F}_i^{ext} - \boldsymbol{F}_i^{int}) + \left(\frac{2}{2 + \alpha \Delta t} \right) \boldsymbol{d}_i - \left(\frac{2 - \alpha \Delta t}{2 + \alpha \Delta t} \right) \boldsymbol{d}_{i-1} \tag{28}$$

Note that using Eq. (28), the displacements at $t + \Delta t$ are calculated by using the mass values and the external and internal forces of the previous time step. An important simplification can be introduced by assuming a diagonal mass matrix. All the calculation in Eq. (28) involves vector operation only.

To start the solution process to calculate $\boldsymbol{d}_1$, $\boldsymbol{d}_{-1}$ is needed and it is given as

$$\boldsymbol{d}_{-1} = \boldsymbol{d}_0 - \Delta t \dot{\boldsymbol{d}}_0 + \frac{1}{2}\Delta t^2 \ddot{\boldsymbol{d}}_0 \tag{29}$$

where $\ddot{\boldsymbol{d}}_0$ can be found as

$$\ddot{\boldsymbol{d}}_0 = \boldsymbol{M}^{-1}(\boldsymbol{F}_0^{ext} - \boldsymbol{F}_0^{int} - \alpha \boldsymbol{M} \dot{\boldsymbol{d}}_0) \tag{30}$$

The explicit time integration is conditionally stable. Its time increment has to be smaller than a limit to avoid the calculations becoming divergent. For multi-degrees of freedom system, the critical time step proposed by Hughes *et al*. (1978, 1979) is given by

$$\Delta t \le \frac{2}{\omega^{\max}} \tag{31}$$

where $\omega^{\max}$ is the maximum frequency of the element. Without going through rigorous studies, the approximated maximum element frequency suggested by Saha and Ting (1983) for the axial mode of vibration is

$$\omega^{\max} = \frac{2}{l}\sqrt{\frac{E}{\rho}} \tag{32}$$

and for the flexural mode of vibration is

$$\omega^{\max} = n^2 \pi^2 \left(\frac{EI_z}{\rho A l^4} \right)^{1/2} \tag{33}$$

where A is the element cross-section area, E the Young's modulus, ρ the mass density, l the element length, I_z the moment of inertia about the major axis of vibration, and $n = 1.2$.

3. Numerical examples and discussion

Example 1. Cantilever beam with a tip load

The proposed numerical model is verified by comparing the numerical solutions with the results obtained by the ANSYS BEAM 23 2-D plastic elements (1998). Fig. 5 shows the geometry, constitutive relation, and load history of the tip-loaded cantilever beam. The numbers of elements and nodes are 20 and 21, respectively. The damping coefficient is $\alpha = 400.0$ sec^{-1}. The Young's modulus is $E_1 = 10.6 \times 10^3$ ksi (7.3034×10^4 MPa), the slope of the linear work hardening is $E_2 = 10.6 \times 10^2$ ksi (7.3034×10^3 MPa), the yield stress is $\sigma_y = 198.75$ ksi (1.3694×10^3 MPa), and the mass density ρ is 2.589×10^{-3} lb·sec^2/in^4 (2.76794×10^4 kg/m^3). The relation of tip vertical displacement versus load is presented in Fig. 6. It is found that the numerical solutions agree well with those of Yu *et al*. (1989) and the results obtained by the ANSYS code.

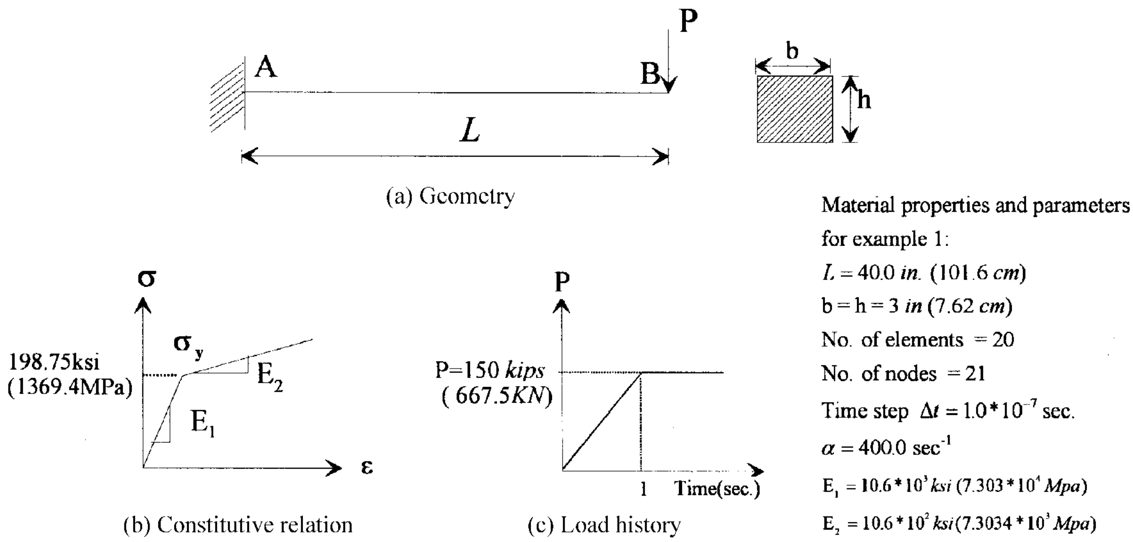

Fig. 5 A tip-loaded cantilever beam

Example 2. Rigid frame subjected to a quasi-static horizontal load

A rigid frame subjected to a static horizontal load is then studied. The geometry, constitutive relation, and load history of a rigid frame are shown in Fig. 7. The cross-section of the member is

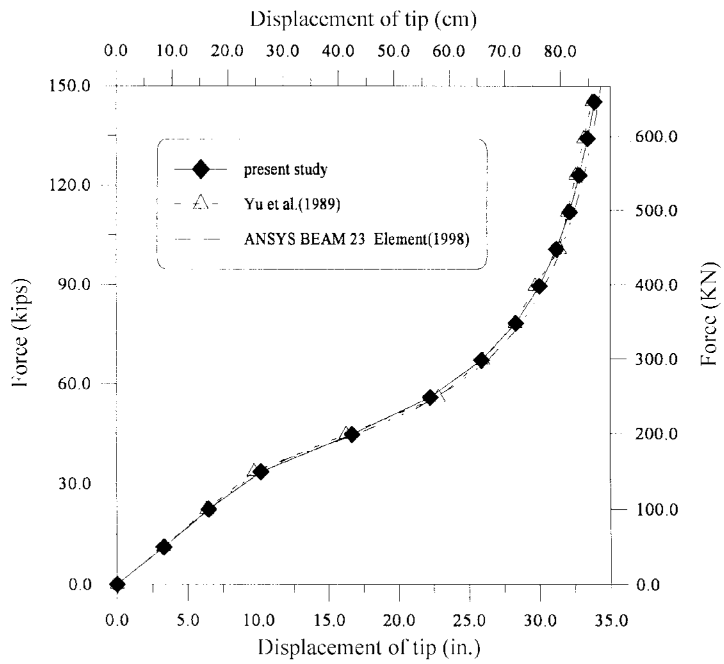

Fig. 6 Load-deflection relation of a tip-loaded cantilever beam

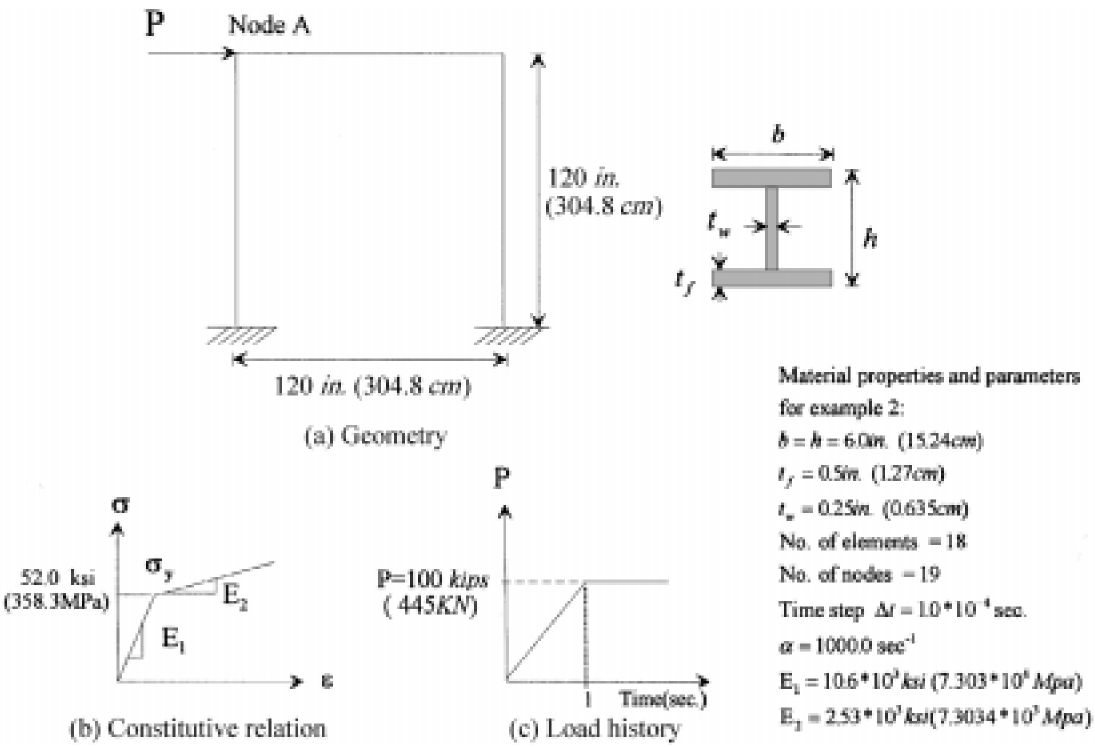

Fig. 7 A rigid frame subjected to a static horizontal load

taken to be *I*-section with width 6 in (15.24 cm), depth 6 in (15.24 cm), flange thickness 0.5 in (1.27 cm), and web thickness 0.25 in (0.635 cm). The numbers of elements and nodes are chosen as 18 and 19, respectively. The damping coefficient is $\alpha = 1000.0$ sec^{-1}. The Young's modulus is $E_1 = 10.6 \times 10^3$ ksi (7.3034×10^4 MPa), the slope of the linear work hardening is $E_2 = 2.53 \times 10^3$ ksi (1.7431×10^4 MPa), the yield stress is $\sigma_y = 52.0$ ksi (358.28 MPa), and the mass density ρ is 2.589×10^{-3} lb·sec^2/in^4 (2.76794×10^4 kg/m^3). The relation of horizontal displacement versus load is presented in Fig. 8. It is found that the numerical results also agree satisfactorily with the results obtained by the ANSYS code. The deformed shape of this frame is shown in Fig. 9. One can observe the characteristic of large displacement and its agreement with the result obtained by ANSYS code.

Example 3. Rigid frame subjected to a dynamic horizontal load

A rigid frame subjected to a dynamic horizontal load is further investigated. The geometry, constitutive relation, and load history of a rigid frame are shown in Fig. 10. The kinematic hardening is adopted to account for the Bauschinger effect. The numbers of elements and nodes, the Young's modulus, the slope of the linear work hardening, the yield stress, and the mass density are the same as the previous one. The relation of horizontal displacement versus time is presented in Fig. 11. It is also found that the numerical results agree satisfactorily with the results obtained by the ANSYS code.

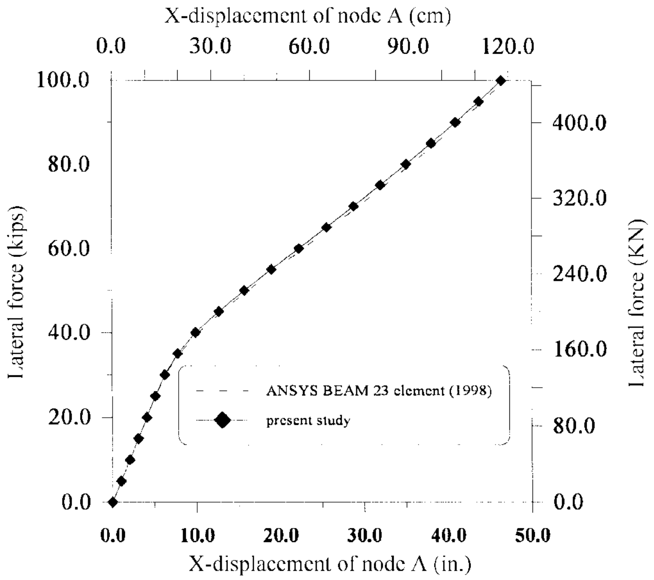

Fig. 8 Load-deflection relation of a rigid frame subjected to a static horizontal load

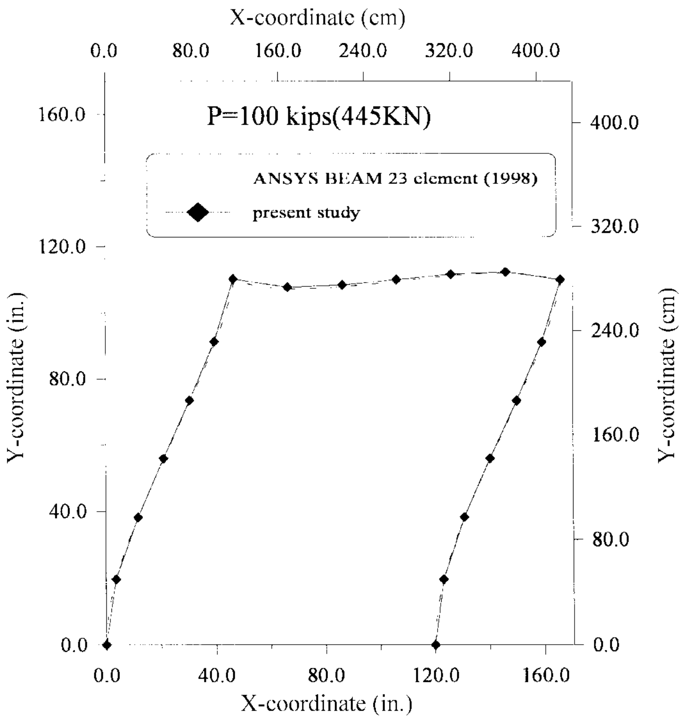

Fig. 9 Deformed shape of a rigid frame subjected to a static horizontal load

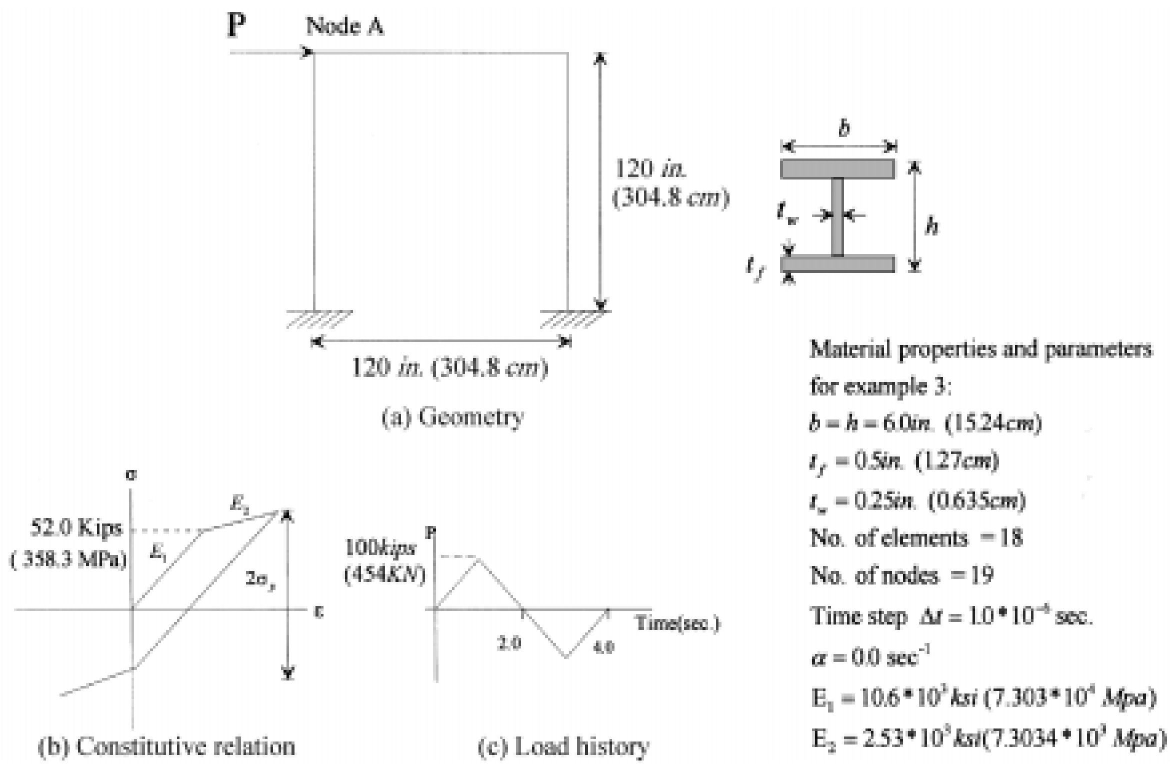

Fig. 10 A rigid frame subjected to a dynamic horizontal load

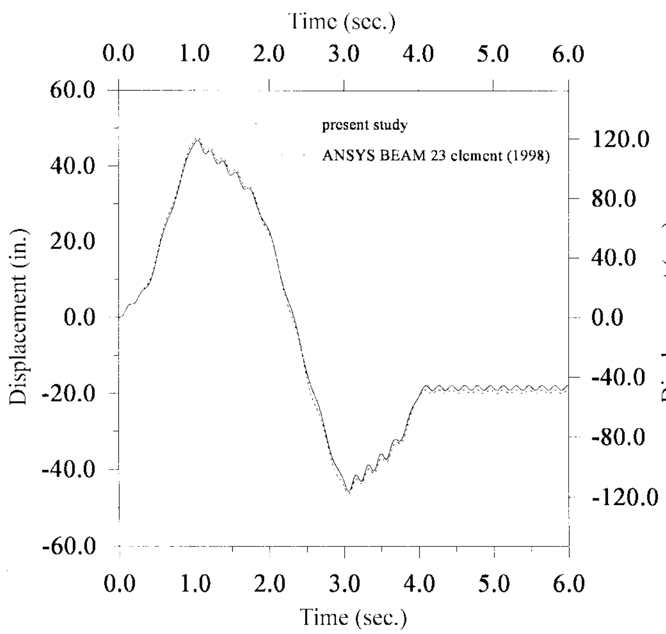

Fig. 11 Displacement-time relation of a rigid frame subjected to a dynamic horizontal load

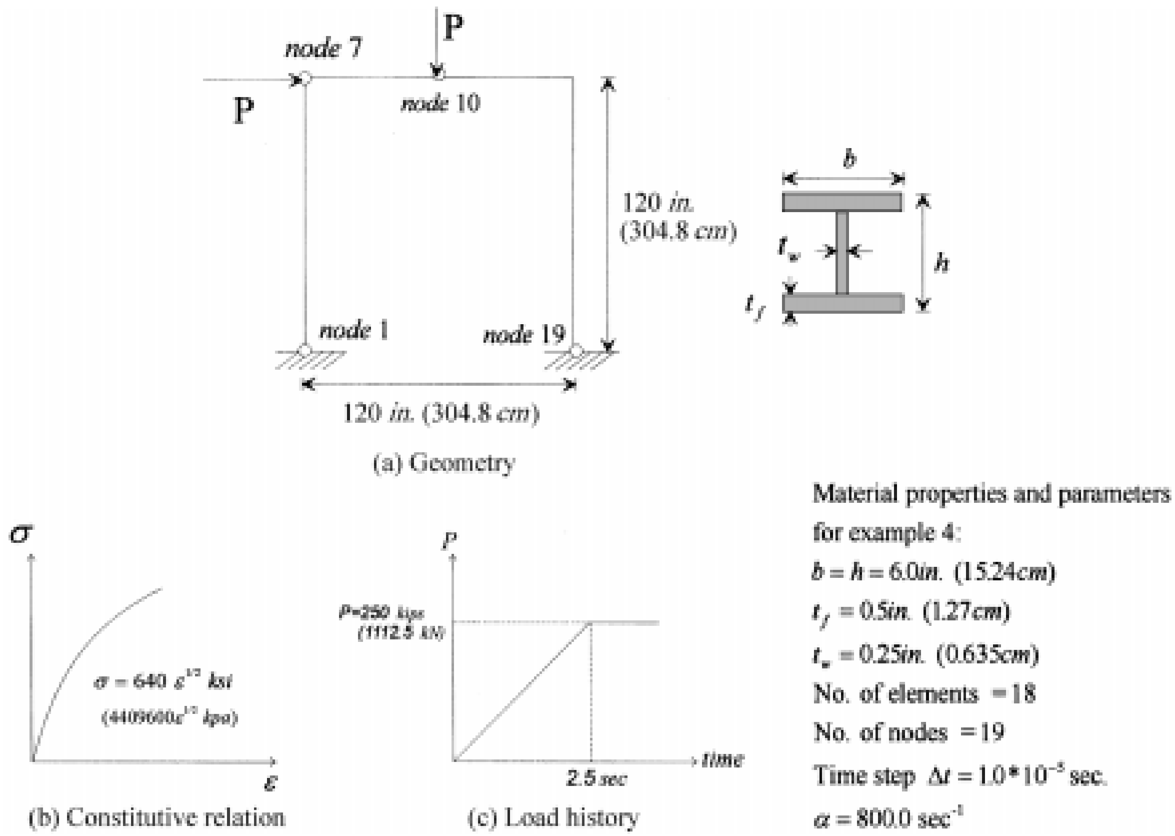

Fig. 12 A nonlinear rigid frame subjected to static horizontal and vertical loads

Example 4. Rigid frame subjected to quasi-static horizontal and vertical loads

The numerical model for static and dynamic responses of nonlinear inelastic frame structures is thus verified. A rigid frame with nonlinear material is then investigated. The geometry, constitutive relation, and load history of the rigid frame are shown in Fig. 12. The numbers of elements and nodes are taken to be 18 and 19, respectively. The damping coefficient is $\alpha = 800.0$ sec^{-1}. The nonlinear constitutive relation is

$$\sigma = 640\varepsilon^{\frac{1}{2}} \text{ ksi} \tag{34a}$$

or

$$\sigma = 4.41 \times 10^3 \varepsilon^{1/2} \text{ MPa} \tag{34b}$$

The relations of the horizontal displacement of node 7 versus load and the vertical displacement of node 10 versus load are illustrated in Fig. 13. Fig 14 shows the obviously nonlinear deformed shape of this frame. Referring to Figs. 13 and 14, it is also demonstrated that the present approach is capable of simulating the large deflection of plane frame with nonlinear material.

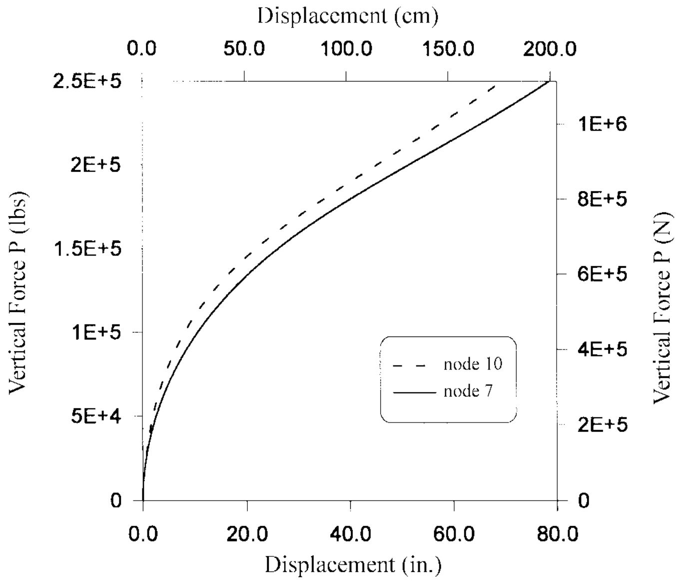

Fig. 13 Load-deflection relation of a nonlinear rigid frame

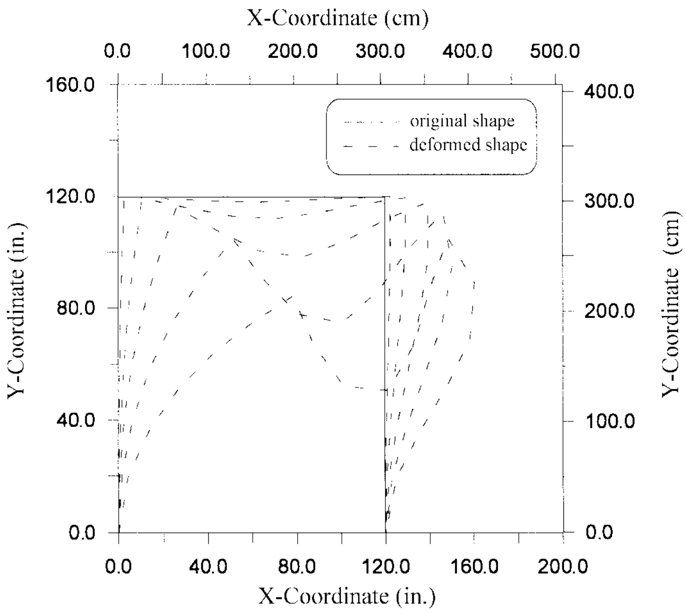

Fig. 14 Deformed shape of a nonlinear rigid frame

4. Conclusions

A convected material frame approach for large deformation combined with the explicit finite formulation is proposed to analyze the inelastic frame structures. This approach is a modification of the co-rotational formulation that has been implemented in many widely used computer codes. The inelastic constitutive relation is derived by using a generalized nonlinear function and the kinematic hardening is adopted. By assuming a lumped mass matrix of diagonal form, the explicit finite element analysis involves only vector assemblage and vector storage. Through the numerical verification with the solutions obtained by the ANSYS code (1998) and the investigation of nonlinear inelastic frame, the convected material frame approach is shown to be accurate and capable of investigating large deflection of inelastic frame structures. This numerical model is proposed to be an alternative efficient approach for nonlinear analysis of inelastic frame structures.

The convected material frame approach has been developed for plane inelastic frame structures in this study. The extension to develop three-dimensional frame elements should be relatively straightforward. Further research to introduce the convected material frame approach for the large deformation of two-dimensional or three-dimensional solid medium is recommended. Due to the limitation of assuming large rotations and small deformations, the co-rotational approach applies only to thin structures, such as beams, plates, and shells. By continuously updating the geometry, the convected material frame approach should be able to handle very large geometry changes of solids.

Acknowledgements

This study is supported by the National Science Council of Republic of China under grant NSC88-2211-E-006-030.

References

ANSYS Release 5.5.1 (1998) ANSYS, Inc., Canonsburg, P. A., U. S. A.

Belytschko, T., and Hsieh, B.J. (1973), "Nonlinear transient finite element analysis with convected coordinates", *Int. J. Numer. Meth. Eng*., **7**, 255-271.

Belytschko, T., and Marchertas, A.H. (1974), "Nonlinear finite element method for plates and its application to dynamics response of reactor fuel subassemblies", Trans. ASME, *J. Pressure Vessel Tech*., **96**(4), 251-257.

Belytschko, T., Schwer, L., and Klein, M.J. (1977), "Large displacement, transient analysis of space frames", *Int. J. Numer. Meth. Eng.*, **11**, 65-84.

Crisfield, M.A. (1990), "A consistent co-rotational formulation for non-linear, three dimensional beam elements", *Compt. Meth. Appl. Mech. Eng*., **81**, 131-150.

Dafalias, Y.F. (1987), "Issues on the constitutive formulation at large elastoplastic deformations, part 1: Kinematics", *Acta Mechanica*, **69**, 119-138.

Dafalias, Y.F. (1988), "Issues on the constitutive formulation at large elastoplastic deformations, part 1: Kinetics", *Acta Mechanica*, **73**, 121-146.

Hsiao, K.M., Horng, H.J., and Chen, Y.R. (1987), "A co-rotational procedure that handles large rotations of spatial beam structures", *Comput. Struct.*, **27**(6), 769-781.

Hsiao, K.M., Lin, J.Y., and Lin, W.Y. (1999), "A consistent co-rotational finite element formulation for geometrically nonlinear dynamic analysis of 3-D beams", *Compt. Meth. Appl. Mech. Eng*., **169**, 1-18.

Hughes, T.J.R., and Liu, W.K. (1978), "Implicit-explicit finite elements in transient analysis: Stability Theory", *J. Appl. Mech.*, ASME, **45**, 371-374.

Hughes, T.J.R., Pister, K.S., and Taylor, R.L. (1979), "Implicit-explicit finite elements in nonlinear transient analysis", *Comput. Methods Appl. Mech, Engng.* **17**(18), 159-182.

Mamaghani, I.H.P., Usami, T., and Mizuno, E. (1996), "Inelastic large deflection analysis of structural steel members under cyclic loading", *Engng. Struct*., **18**(9), 659-668.

Rice, D.L., and Ting, E.C. (1993), "Large displacement transient analysis of flexible structures", *Int. J. Numer. Meth. Eng*, **36**, 1541-1562.

Saha, N., and Ting, E.C. (1983), *Large displacement dynamic analysis of space frames*, EC-SRT-83-5, School of Civil Engineering, Purdue University, IN. U. S. A.

Tang, S.C., Yeung, K.S., and Chon, C.T. (1980), "On the tangent stiffness matrix in a convected coordinate system", *Comput. Struct*., **12**, 849-856.

Wang, B., Lu, G., and Yu, T.X. (1995), "A numerical analysis of the large deflection of an elastoplastic cantilever", *Struct. Engng. Mech*., **3**(2), 163-172.

Wang, Y.K., Shih, C., and Ting, E.C. (1998), *A general curved element for very flexible frames*, CE-ST-1998-001, Department of Civil Engineering, National Central University, Taiwan, R. O. C.

Yang, T.Y., and Saigal, S. (1984), "A simple element for static and dynamic response of beams with material and geometric nonlinearities", *Int. J. Num. Meth. Eng*., **20**, 851-867.

Yu, T.X., Stronge, W.J., and Liu, J.H. (1989), "Large deflections of an elastoplastic strain-hardening cantilever", *J. Appl. Mech.*, ASME, **56**, 737-743.